Mon. Not. R. Astron. Soc. **347,** 29–35 (2004)

# *XMM–Newton* observations of the Perseus cluster – II. Evidence for gas motions in the core

E. Churazov,[1,2⋆] W. Forman,[3] C. Jones,[3] R. Sunyaev[1,2] and H. Böhringer[4]

[1]*Max-Planck-Institut für Astrophysik, Karl-Schwarzschild-Strasse 1, 85741 Garching, Germany*
[2]*Space Research Institute (IKI), Profsoyuznaya 84/32, Moscow 117810, Russia*
[3]*Harvard-Smithsonian Centre for Astrophysics, 60 Garden St., Cambridge, MA 02138, USA*
[4]*MPI für Extraterrestrische Physik, PO Box 1603, 85740 Garching, Germany*

Accepted 2003 September 11. Received 2003 September 10; in original form 2003 July 15

**ABSTRACT**

The 5–9 keV spectrum of the inner ∼100 kpc of the Perseus cluster measured by *XMM–Newton* can be well described by an optically thin plasma emission model as predicted by the APEC code, without any need for invoking a strong Ni overabundance or the effects of resonant scattering. For the strongest 6.7-keV line of He-like iron, the optical depth of the cluster, calculated using observed density, temperature and abundance profiles, is of the order of 3. The lack of evidence for resonant scattering effects implies gas motion in the core with a range in velocities of at least half of the sound velocity. If this motion has the character of small-scale turbulence, then its dissipation would provide enough energy to compensate for radiative cooling of the gas. The activity of the supermassive black hole at the centre of the cluster may be the driving force of the gas motion.

**Key words:** galaxies: clusters: individual: Perseus – cooling flows – X-rays: galaxies: clusters.

## 1 INTRODUCTION

The X-ray emission of the hot gas in galaxy clusters is usually modelled as emission by an optically thin plasma. The assumption that the cluster gas is optically thin is certainly valid for the continuum emission, but for the strongest resonant lines the cluster can be moderately thick (e.g. Gilfanov, Sunyaev & Churazov 1987). Resonant scattering causes changes in line intensities relative to the continuum, thus affecting measurements of the heavy element abundances (Gilfanov et al. 1987; Shigeyama 1998), and producing polarization of the line flux at the level of ∼10 per cent (Sazonov, Churazov & Sunyaev 2002). For a typical rich cluster we can expect the resonant scattering to be especially important for the He-like iron $K_\alpha$ line at 6.7 keV. It is most convenient to search for resonant scattering effects by comparing the flux from this line with the flux of the He-like iron $K_\beta$ line at 7.9 keV. In particular, for the Perseus cluster, Molendi et al. (1998) and Akimoto et al. (1997, 1999) argued that an anomalously high ratio of the He-like iron $K_\beta$ and $K_\alpha$ lines hints at the importance of resonant scattering. The 7.9-keV line of iron is, however, blended with the He-like nickel $K_\alpha$ line and the anomalous line ratio may be interpreted as evidence for an enhanced Ni abundance (Dupke & Arnaud 2001). The role of resonant scattering has also been discussed for other objects, in particular M87 (Böhringer et al. 2001; Mathews, Buote & Brighenti 2001; Matsushita, Finoguenov & Böhringer 2003) and NGC 4636 (Xu et al. 2002).

Below we use an *XMM–Newton* 50-ks observation of the Perseus cluster to assess the possible role of resonant scattering. The detailed description of the data and the analysis procedure are given in Churazov et al. (2003).

The structure of the paper is as follows. In Section 2 we simulate the effect of resonant scattering on the radial profiles of the line intensities. In Section 3 we compare the results of the observations with the simulations. In Section 4 we set a lower limit on the level of gas turbulence, which in the context of this paper means differential gas flows on scales smaller than ∼100 kpc. In Section 5 we briefly argue that the central abundance decrement may not be a strong argument in favour of resonant scattering. Implications of turbulent motions on the thermal balance of the gas are discussed in Section 6. The final section summarizes our findings.

Throughout the paper we use $H_0 = 70$ km s$^{-1}$ Mpc$^{-1}$.

## 2 RESONANT SCATTERING

The radial dependence of the electron density $n_e$ and temperature $T_e$ of the gas in the Perseus cluster is taken from Churazov et al. (2003), rescaled to $H_0 = 70$ km s$^{-1}$ Mpc$^{-1}$, namely

$$n_e = \frac{4.6\times10^{-2}}{\left[1+(r/57)^2\right]^{1.8}} + \frac{4.8\times10^{-3}}{\left[1+(r/200)^2\right]^{0.87}}\ \mathrm{cm}^{-3} \quad (1)$$

and

$$T_e = 7\frac{\left[1+(r/71)^3\right]}{\left[2.3+(r/71)^3\right]}\ \mathrm{keV}, \quad (2)$$

where $r$ is measured in kpc.

⋆E-mail: churazov@mpa-garching.mpg.de

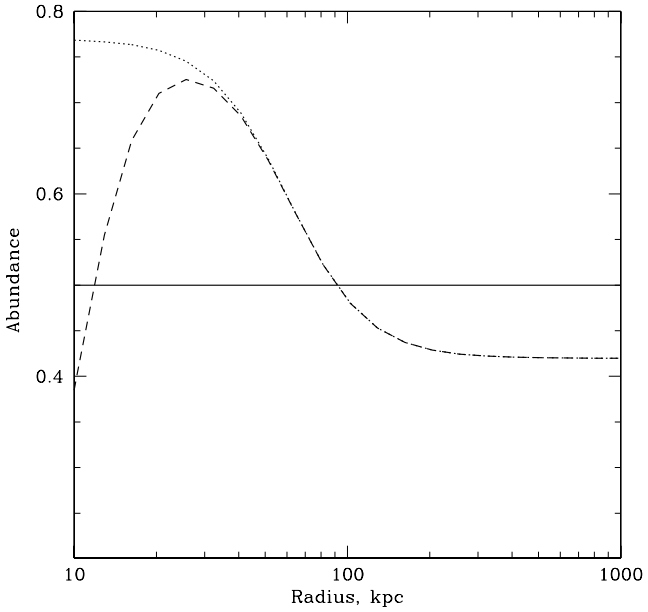


**Figure 1.** Three radial abundance profiles used in the simulations.

For abundances we consider three possible radial behaviours: (a) constant abundance, (b) abundance declining with radius and (c) abundance peaking at the radius of ∼50 kpc and declining both towards smaller or larger radii as shown in Fig. 1. The last functional form is closest to the radial abundance profile derived from the deprojection analysis of the *Chandra* and *XMM–Newton* observations (Schmidt, Fabian & Sanders 2002; Churazov et al. 2003) under the assumption of a single-temperature optically thin plasma emission model. The abundance ratios used are those of Anders & Grevesse (1989). Using these data we calculated an optical depth from the centre of the cluster up to a radius of 1 Mpc, $\tau = \int n_{\rm i}\sigma_0\,{\rm d}r$, where $n_{\rm i}$ is the ion concentration and the cross-section for a given ion is

$$\sigma_0 = \frac{\sqrt{\pi}hr_{\rm e}cf}{\Delta E_{\rm D}}, \tag{3}$$

where

$$\Delta E_{\rm D} = E_0\left(\frac{2kT_{\rm e}}{Am_{\rm p}c^2} + \frac{V_{\rm turb}^2}{c^2}\right)^{1/2} = E_0\left[\frac{2kT_{\rm e}}{Am_{\rm p}c^2}(1 + 1.4AM^2)\right]^{1/2}. \tag{4}$$

In the above equations $E_0$ is the energy of a given line, $A$ is the atomic mass of the corresponding element, $m_{\rm p}$ is the proton mass, $V_{\rm turb}$ is the characteristic turbulent velocity, $M$ is the corresponding Mach number, $r_{\rm e}$ is the classical electron radius and $f$ is the oscillator strength of a given atomic transition. The wavelengths and absorption oscillator strengths are taken from the compilation of Verner, Verner & Ferland (1996). The ionization equilibrium is that of Mazzotta et al. (1998). The set of Fe lines with an optical depth larger than 0.2 (for $M = 0$) is given in Table 1. From this table it is clear that (i) the 6.7-keV line of He-like iron is by far the most optically thick line for the case of pure thermal broadening and (ii) strong turbulence makes resonant scattering effects negligible for all lines as emphasized by Gilfanov et al. (1987). For other types of abundance profiles, the main result is the same; the 6.7-keV line has an optical depth of the order of 3 and accounting for turbulence reduces the optical depth to values smaller than 1.

**Table 1.** Optical depth (from $r = 0$ to $r = 1$ Mpc) to resonant scattering for a set of X-ray lines. The temperature and density profiles are give by equations (1) and (2). The abundance is constant with radius at 0.5 solar. Two values are quoted: for pure thermal line broadening ($M = 0$) and for strongly turbulent gas ($M = 1$). Only the lines with an optical depth greater than 0.2 (for $M = 0$) are listed.

| Ion | Energy (keV) | $\tau$ $M = 0$ | $\tau$ $M = 1$ |
|---|---|---|---|
| Fe XXIII | 0.093 | 0.70 | 0.08 |
| Fe XXIII | 1.129 | 0.26 | 0.03 |
| Fe XXIV | 1.163 | 0.39 | 0.04 |
| Fe XXIV | 1.168 | 0.78 | 0.09 |
| Fe XXV | 6.700 | 2.79 | 0.31 |
| Fe XXVI | 6.973 | 0.20 | 0.02 |
| Fe XXV | 7.881 | 0.46 | 0.05 |

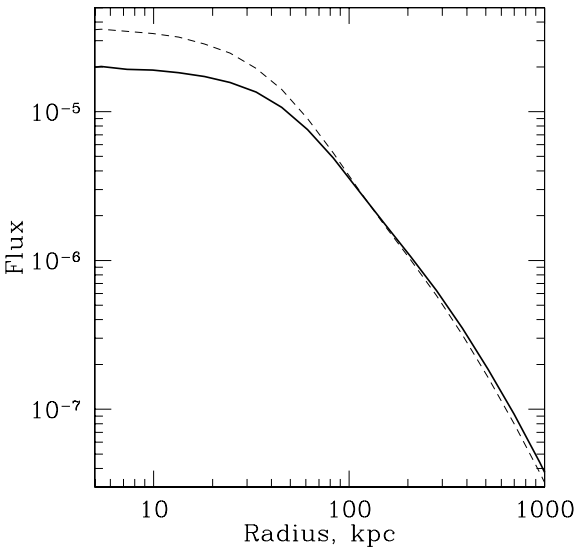


**Figure 2.** Radial profiles of the He-like iron $K_\alpha$ line (for the flat abundance profile) with (thick solid line) and without (dashed line) the effect of resonant scattering. Resonant scattering suppresses the line intensity in the core and redistributes line photons to larger radii.

The resonant scattering has been modelled using a Monte Carlo approach. The cluster has been divided into concentric shells and line emissivities have been assigned to each shell using the APEC v1.3.0 results (Smith et al. 2001). The scattering of photons was accounted for by assuming a complete energy redistribution and dipole scattering phase matrix. The latter assumption is motivated by the fact that we are interested primarily in the He-like iron resonant line, which has a pure dipole scattering phase matrix (see the discussion in Sazonov et al. 2002). The escaping photons are accumulated into separate bins, according to their projected distance from the cluster centre. The modification of the 6.7-keV line radial brightness profile due to resonant scattering (for the case of a flat abundance profile) is shown in Fig. 2. As expected, resonant scattering suppresses the line intensity in the core and raises the line intensity in the cluster outskirts. More illustrative is the ratio of the profiles with and without resonant scattering taken into account, which we show in Fig. 3 for all three abundance profile models. In spite of the different abundance distributions, this plot shows that the net effect is very

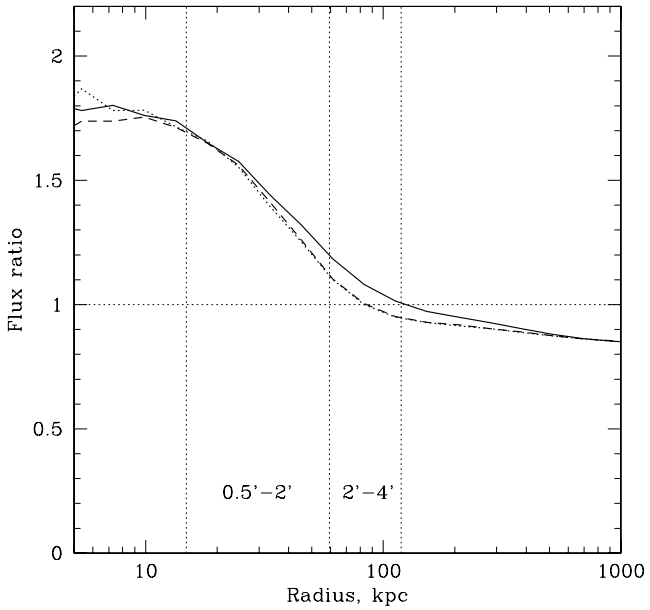


**Figure 3.** Ratio of the 6.7-keV radial brightness profiles without accounting for resonant scattering to the profiles including the effect of resonant scattering. The three curves correspond to the three models of the abundance profiles shown in Fig. 1. Dotted vertical lines show the two regions used for spectra extraction.

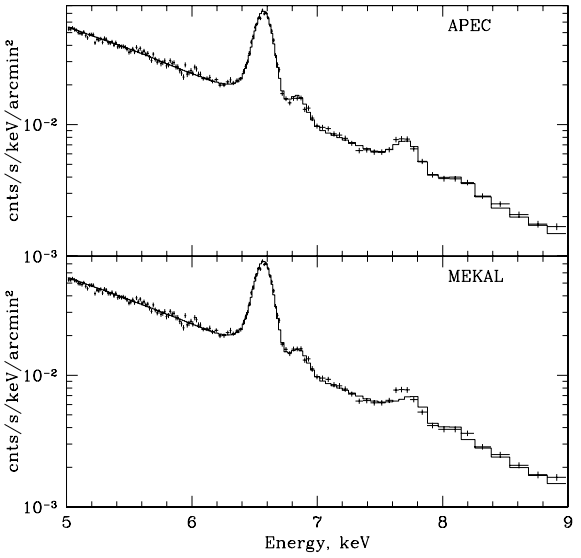


**Figure 4.** The 5–9 keV spectrum of the 30 arcsec to 2 arcmin annulus centred on NGC 1275 and fitted with APEC and MEKAL models.

similar for all three cases; the flux in the line is suppressed by a factor of up to ∼2 within the inner 100-kpc region and is enhanced by ∼10–20 per cent outside this region.

## 3 SPECTRA

Obviously the easiest way to reveal the effect of resonant scattering is to derive the line ratios for the central region. The He-like iron $K_\alpha$ and $K_\beta$ lines are ideally suited for this purpose because both lines are due to the same ion of iron. Guided by Fig. 3 we accumulated MOS spectra for two annuli, 0.5–2 and 2–4 arcmin, centred on NGC 1275. The inner 0.5-arcmin region was excluded in order to avoid possible contamination from the NGC 1275 nucleus. The spectrum from 5 to 9 keV was fitted with the APEC (Smith et al. 2001) and MEKAL (Mewe, Gronenschild & van den Oord 1985; Mewe, Lemen & van den Oord 1986; Kaastra 1992; Liedahl, Osterheld & Goldstein 1995) models in XSPEC v.11.2 (Arnaud 1996) and is shown in Fig. 4. Temperature, heavy metal abundances (with the abundance ratios of Anders & Grevesse 1989) and redshift were free parameters of the models. We can see that for the MEKAL model there is a clear excess on the left wing of the He-like iron $K_\beta$ line, where the He-like nickel $K_\alpha$ line(s) is blended with the iron line. In order to remove this discrepancy we have to either raise the nickel abundance above the standard Ni to Fe ratio (Anders & Grevesse 1989) by a factor of ∼2 or assume that the 6.7-keV complex is suppressed by resonant scattering, thus causing peculiarities in the observed line ratio. On the other hand, the most recent APEC v1.3.0 model provides an almost perfect fit to the whole 5–9 keV portion of the spectrum. A very similar situation is seen for the spectrum of the 2–4 arcmin annulus. In what follows we assume that we can rely on the predictions of the newest APEC model, which has a significantly richer set of lines in the region of interest. The best-fitting temperature and abundance values for the two annuli are $T_e = 4.29 \pm 0.05$ keV, $Z = 0.501 \pm 0.007$ relative to the solar abundance (Anders & Grevesse 1989) and $T_e = 5.18 \pm 0.06$, $Z = 0.446 \pm 0.007$. The values of temperature are higher than we would infer from fitting a broader 0.5–9 keV spectral band, which is expected for projected spectra, given the radial dependence of the temperature in the Perseus cluster (see equation 2).

The best-fitting value of the abundance for the 5–9 keV spectrum is, of course, dominated by the contribution of the 6.7-keV line. We fixed all parameters (except abundance) at their best-fitting values and recalculated the abundance, first ignoring part of the spectrum containing the 6.7-keV complex and secondly ignoring the part containing 7.9-keV complex. Because only the 6.7-keV complex is affected by resonant scattering, the different values of abundance in the two fits would indicate an important role for scattering. The ratio of abundances calculated this way is shown in Fig. 5 with two crosses (for two annuli). Resonant scattering is expected to increase the ratio of abundances well above unity for the inner annulus. However, the observed ratio is consistent with unity, indicating that any effects from resonant scattering are small.

Finally, we have demonstrated that projection effects do not significantly affect the determination of the spectral parameters by using the outer 2–4 arcmin annulus as a background for the inner 0.5–2 arcmin annulus. The resulting spectrum has a lower best-fitting temperature ∼3.8 keV, as expected, but the line flux ratio again does not show any obvious anomalies.

## 4 ROLE OF GAS MOTIONS

The resonant $K_\alpha$ He-like iron line contribution to the 6.7-keV (6.6–6.8 keV) complex varies from 40 to 52 per cent for the gas temperature range from 3 to 5 keV. Therefore, suppression of the resonant line flux in the inner regions due to resonant scattering would strongly affect the intensity of the whole complex. On the other hand, the 6.9- and 7.9-keV complexes can be treated as effectively optically thin. The good fit of the spectra with the APEC model of an optically thin plasma with the solar mix of heavy elements can be considered as an indication that the resonant scattering effects are suppressed. As noted by Gilfanov et al. (1987) turbulent motions of the gas may significantly reduce the optical depth of the lines. The effect is especially strong for heavy elements, which have thermal velocities much smaller than the sound velocity of the gas. For

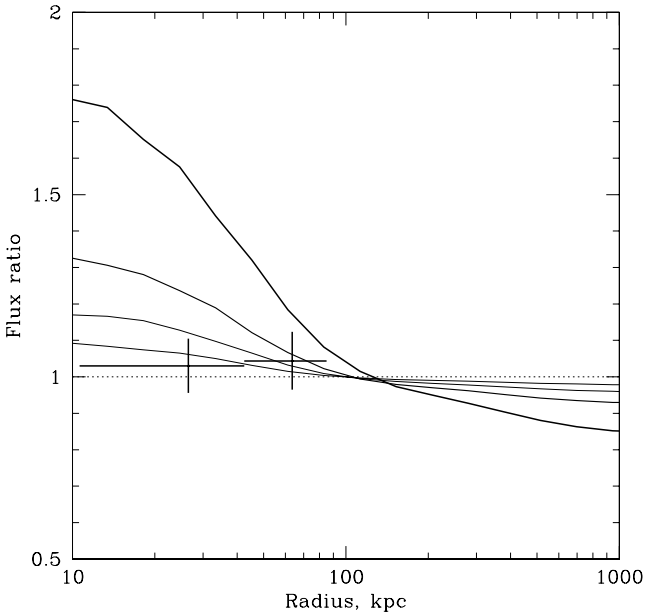


**Figure 5.** Influence of turbulence on the strength of the resonant scattering effect. The plot shows the same ratio as in Fig. 3 for the flat abundance profile, but calculated for Mach numbers of 0, 0.25, 0.5 and 1 (from top to bottom). For comparison, crosses show the ratio of heavy element abundances obtained ignoring parts of the spectrum containing the 6.7-keV and 7.9-keV complexes. Given that the resonant $K_\alpha$ line of He-like iron contributes about 50 per cent to the 6.6–6.8 keV complex of lines, the measured abundance ratio is consistent with the curves for Mach number $\geqslant$0.5.

example, for the 6.7-keV iron line, the inclusion of turbulent motions (parametrized through the effective Mach number in equation 4) would reduce the optical depth to $\sim$0.4 for a Mach number of 1. In Fig. 5, we show the simulated ratios of the radial profiles of the 6.7-keV line with and without the effect of resonant scattering for Mach numbers of 0, 0.25, 0.5 and 1.

## 5 CENTRAL ABUNDANCE HOLE

Single-temperature fits to the azimuthly averaged projected spectra of the Perseus cluster yield an abundance 'hole' in the very core (central $\sim$1 arcmin) of the cluster (e.g. Schmidt et al. 2002; Churazov et al. 2003). It is, of course, attractive to attribute this decrease in abundance to resonant scattering, because abundance measurements are mostly affected by the strongest lines which typically have the largest optical depths. The high signal-to-noise ratio accumulated during the *XMM–Newton* observations of the Perseus cluster allows us to make a two-dimensional map of the 6.7-keV line intensity. Fig. 6 (left-hand panel) shows the projected map of the 6.7-keV line equivalent width. The 5–8 keV band of the projected spectra was approximated as a linear combination of three components: two bremsstrahlung spectra with temperatures of 2 and 6 keV and a Gaussian line at 6.7 keV (redshifted to the cluster distance). The very central region (the circle with 20-arcsec radius centred at NGC 1275) has been excised from the analysis to avoid contamination by the active galactic nucleus (AGN) flux. The equivalent width of the line was calculated by applying similar adaptive smoothings to the intensities of the line and the continuum (sum of two bremsstrahlung components) and calculating the ratio. The size of the smoothing window was chosen to provide an effective signal-to-noise ratio of 80, calculated using the total number of counts from 5 to 8 keV. The image shows (i) an overall increase in the equivalent width towards the centre of the cluster, (ii) a decrease in the equivalent width in the central $\sim$1-arcmin region and (iii) a low equivalent width horseshoe shaped region to the west. Because the equivalent width of the line is temperature-dependent, we have calibrated this dependence using a set of simulated APEC spectra with different temperatures and a fixed heavy element abundance and applying a similar procedure for equivalent width determination. Using the resulting conversion factor (from equivalent width to abundance) and the temperature map calculated with the same adaptive smoothing procedure, we converted the equivalent width map into an abundance map (Fig. 6, right-hand panel). The low equivalent width region to the west of the cluster centre is apparently the result of higher gas temperature in this region (see Churazov et al. 2003), because in the abundance map this feature is absent. The central 'hole' is present both in the equivalent width and the abundance map, although detailed structures are different in the two maps, because of the complicated temperature structure of the inner region.

The central part ($8 \times 8$ arcmin$^2$) of the abundance map is shown in Fig. 7 along with the surface brightness image of the same region. Contours in both images show the abundance at the level of 0.4 solar. We can see that the inner part of the abundance hole roughly traces the region occupied by the inner radio lobes (Böhringer et al. 1993; Fabian et al. 2000) which correspond to areas of low X-ray surface brightness to the north and south of the nucleus. This morphological similarity suggests that the abundance 'hole' is related to the activity of the AGN rather than to resonant scattering. For instance, radio lobes may push the gas with the highest abundance away from the nucleus forming a shell-like distribution of highly enriched gas. The details of the abundance distribution in this region and discussion of realistic models are beyond the scope of this paper. Given that the size of the region is rather small and there is a bright AGN at the very centre, long *Chandra* observations would provide better data for careful study of the abundance distribution. We conclude, however, that a central abundance hole is not a reliable indication that resonant scattering is important in Perseus and it is likely that other physical mechanisms play a role.

## 6 DISCUSSION

With our parametrization of the turbulence through the effective Mach number in equation (4), the energy in turbulent motions is approximately related to the thermal energy of the gas as $\epsilon_{\rm turb} \approx 0.7M^2\epsilon_{\rm th}$. A lack of visible effects of resonant scattering suggests that $M$ is at least 0.5. Therefore, turbulent motions contain at least 20 per cent of the thermal energy of the gas. Subsonic turbulence is not very efficient in generating sound waves (e.g. Landau & Lifshitz 1963) and we can assume that a significant fraction of this energy will be dissipated locally and will go into heat. The dissipation timescale can be estimated as the eddy turnaround time times a factor $f$ of the order of a few. Thus, a rough estimate of the heating rate due to dissipation of turbulence can be written as

$$\frac{\epsilon_{\rm turb}}{f(l/Mc_{\rm s})} \approx \frac{0.7}{f}M^3\frac{\epsilon_{\rm th}}{l/c_{\rm s}} \approx \frac{\epsilon_{\rm th}}{2\times10^8\,{\rm yr}}, \quad (5)$$

where $l$ is the characteristic eddy size, $c_{\rm s}$ is the sound velocity. For estimates we set $l = 10$ kpc, $M = 0.5$ and $f = 3$. This value can be compared with the cooling rate which is set by the thermal energy and the cooling time which is of the order of 0.5 Gyr for the gas density and temperature typical of the Perseus core. Thus, if the characteristic spatial scale of turbulent eddies is comparable to or

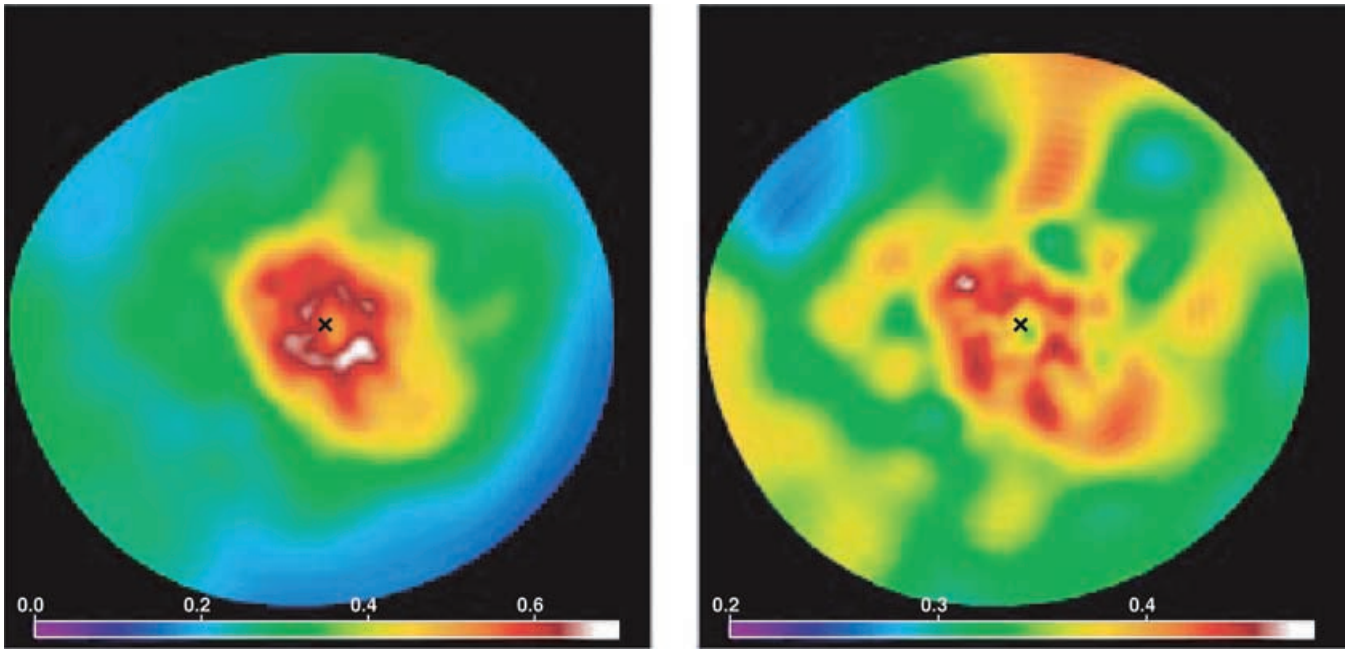


**Figure 6.** Left: Adaptively smoothed map of the 6.7-keV line equivalent width in units of keV. The image size is 20 × 20 arcmin$^2$. The cross marks the position of NGC 1275. Right: The abundance map (in units of solar abundance) calculated from the equivalent width map using the projected temperature map. This figure can be seen in colour in the on-line version of the journal in *Synergy*.

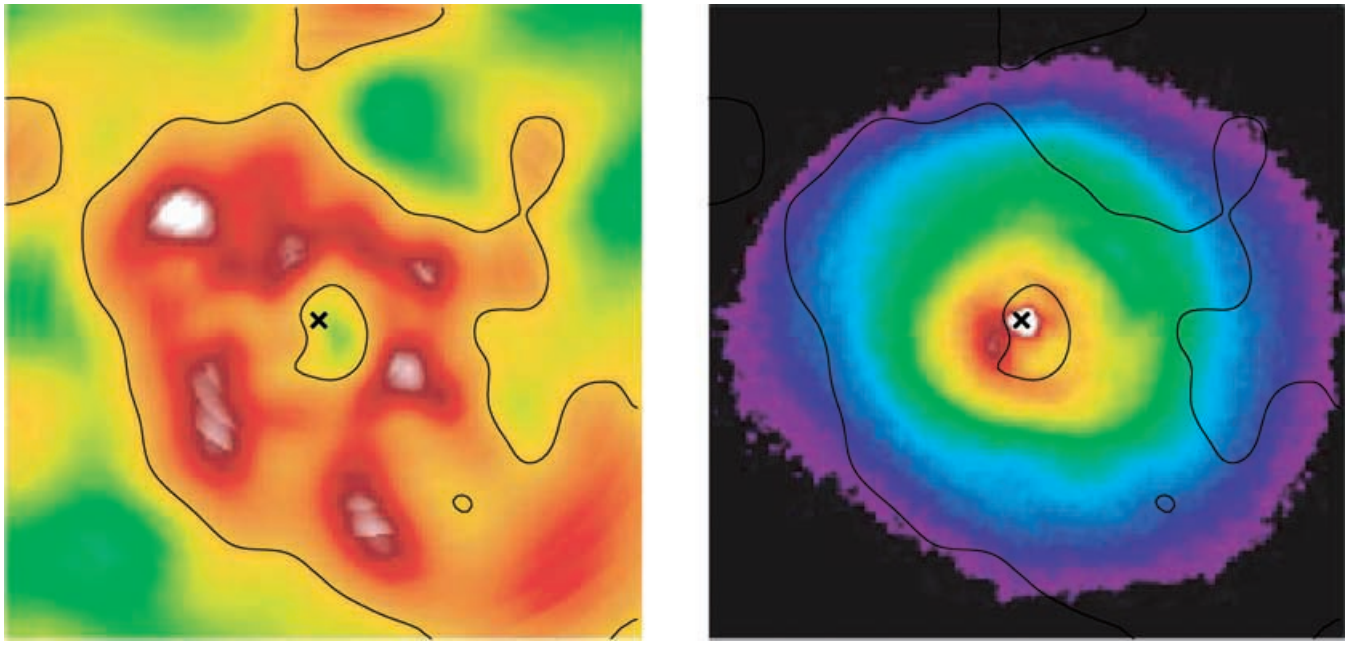

**Figure 7.** Left: Central 8 × 8 arcmin$^2$ part of the iron abundance map. Right: Surface brightness distribution of the same region in the 0.3–5 keV band. Contours in both images show the abundance at the level of 0.4 solar. The inner part of the abundance hole approximately covers two regions of low surface brightness to the north and south of the nucleus that correspond to the two radio lobes (Böhringer et al. 1993; Fabian et al. 2000). This figure can be seen in colour in the on-line version of the journal in *Synergy*.

less than ∼10 kpc, then the present level of turbulent dissipation should be sufficient to compensate for the gas cooling losses.

There are at least two obvious sources of turbulence: mergers and the activity of the central supermassive black hole. The numerical simulations have shown that mergers can induce long-lived (of the order of Gyr) eddies (e.g. Norman & Bryan 1999) even in cluster cores. The surface brightness and gas temperature structures in Perseus suggest recent merger activity (e.g. Furusho et al. 2001). The scale of merger induced eddies is probably rather large and this reduces the dissipation rate. On the other hand, activity of the supermassive black hole can induce turbulence on a smaller scales through the mechanical action of the outflows (Churazov et al. 2001,

2002; Reynolds, Heinz & Begelman 2002; Brüggen & Kaiser 2002). Judging from the size of the observed radio lobes in the Perseus cluster (Böhringer et al. 1993; Fabian et al. 2000) we can expect the size of the generated eddies to be of the order of 10 kpc, i.e. sufficiently small to dissipate their energy quickly (compared to the time-scale for radiative cooling).

The above analysis is simplified by the assumption that the same level of turbulence, expressed through the effective Mach number, is applicable to all radii. We cannot prove, however, with the present data that the gas velocities indeed vary on spatial scales as small as 10 kpc, nor is it possible to show that the velocity field can be characterized as turbulent motion. The conservative conclusion is therefore that the data are consistent with small-scale turbulence characterized by a velocity of the order of half the sound speed, although larger spatial scale velocity variations (up to ∼50–100 kpc) cannot be excluded. Comparable gas velocities are found in the numerical simulations of cluster formation (e.g. Frenk et al. 1999), although the central parts of clusters with cool cores may have properties different from the bulk of the cluster gas. The profile of a resonant line, broadened by large-scale motions and the turbulent cascade, has been recently calculated by Inogamov & Sunyaev (2003). While the profile differs from a simple Gaussian shape, the net effect on the optical depth in the line core is comparable. We note also that pure radial differential motions – e.g. sound waves coming from the very central region, as in the picture suggested by Fabian et al. (2003a,b) – would also produce a similar reduction in the optical depth of the lines. The dissipation rate for this (predominantly radial) motion crucially depends on the viscosity of the gas (Fabian et al. 2003a,b). For less regular motion patterns, equation (5) gives a reasonable estimate of the dissipation time-scales for all values of the viscosity below a certain value (in the limit of large Reynolds numbers). For very high viscosities (low Reynolds numbers) the time-scale for dissipation will be even shorter.

Assuming that the gas velocities do vary randomly on spatial scales of the order of 10 kpc, we can estimate the impact of these motions on the radial distribution of heavy elements. In the simplest approximation, we can estimate the turbulent transport of heavy elements via the diffusion coefficient on spatial scales larger than the characteristic size of the eddies:

$$D \sim \frac{1}{3} v_t l = \frac{1}{3} M c_s l. \tag{6}$$

The characteristic time for diffusion over regions of size $X$, e.g. 100 kpc, is

$$t \sim \frac{X^2}{D} = 6 \times 10^9 \left(\frac{X}{100\,\mathrm{kpc}}\right)^2 \times \left(\frac{l}{10\,\mathrm{kpc}}\right)^{-1} \left(\frac{M c_s}{500\,\mathrm{km\,s^{-1}}}\right)^{-1} \mathrm{yr}. \tag{7}$$

Thus, for our choice of typical eddy size and turbulent velocity, the metals are not transported outside a region much larger than 100 kpc during the lifetime of the cluster. The central abundance (adopting the abundance profile with a maximum at the centre as shown in Fig. 1), however, does drop substantially on time-scales of approximately 1–2 Gyr and has to be replenished by some mechanism; see Böhringer et al. (2003) for implications of abundance gradients on the properties of the cool core clusters. Given the different dependence of the turbulent diffusion coefficient (equation 7) and the rate of dissipation (equation 5) on the spatial scales of eddies and characteristic velocities, the importance of these two processes will differ. For some combinations of parameters (in particular, for small eddies), the heating rate is high while the impact of turbulent transport may be limited. Because, at present, these values are highly uncertain, it is difficult to prove that such a situation is indeed taking place in Perseus.

There are several additional caveats associated with the above analysis which are necessary to mention. First of all, there are still issues to be resolved in the plasma emission models, in particular near the He-like Ni $K_\alpha$ line. Compared to the MEKAL version included in XSPEC (version 11.2.0), the APEC code has an updated set of major line energies and atomic physics (Smith et al. 2001, see also http://cxc.harvard.edu/atomdb). For the MEKAL model, however, the best descriptions of the spectra are obtained when Ni is overabundant (Dupke & Arnaud 2001; Gastaldello & Molendi 2003) rather than by effects of resonant scattering. It seems therefore that, even though the predictions of the two codes differ, both codes favour a minimal role for resonant scattering. Secondly, the presence of multitemperature plasma in the Perseus core and projection effects make the straightforward interpretation of simple single-temperature fits to the projected spectra questionable. Finally, the *XMM–Newton* observation of the Perseus cluster was affected by increased background (see Churazov et al. 2003, for details) which might slightly affect the spectral parameters. We believe however that all these problems should not affect our estimate that the random gas velocities in the Perseus cluster core are a substantial fraction of the gas sound speed.

The presence of differential motions and the role of the resonance scattering in the Perseus core can be verified in future X-ray observations. The most straightforward way would be the measurements of the linewidth with calorimeters (ASTRO-E2, Constellation-X, XEUS). Resonant lines are broadened both by the resonant scattering (e.g. Gilfanov et al. 1987) and the differential motions (e.g. Inogamov & Sunyaev 2003; Sunyaev, Norman & Bryan 2003), while the width of the forbidden or intercombination lines is affected only by differential motions. Comparison of the linewidths would provide an important test on the contribution of the resonant scattering. At the temperature of 4 keV, the pure Doppler width of the iron 6.7-keV resonant line is of the order of 4 eV (FWHM) or $\sim$200 km s$^{-1}$. Resonant scattering (for an optical depth of the order of 3) would double the width of the resonant line (Gilfanov et al. 1987). These values are comparable with the ASTRO-E2 energy resolution and could be measured. The shape of the line and mapping of the line centroid energy over the central region will help to identify the characteristic size of the eddies (e.g. Inogamov & Sunyaev 2003).

A more demanding test for the presence of resonant scattering would be the measurements of the polarization of the line flux (Sazonov et al. 2002). The expected degree of polarization for the central region is, however, small (at the level of a few per cent) which makes a detection or meaningful upper limits problematic for future polarimetric projects.

The third possibility is related to $H_\alpha$ filaments observed in the core of the Perseus cluster. If the filaments are constructed from extremely small clouds as suggested by Fabian et al. (2003b), which are dragged by the flow of the hot gas, then we can obtain a direct estimate of the gas velocity spread ∼300 km s$^{-1}$ (e.g. Conselice, Gallagher & Wyse 2001) and the characteristic scales of the eddies (∼10 kpc) from the optical data. We note that, if individual clouds are not very small, have a temperature of $10^4$ K and are in pressure equilibrium with the ambient hot gas at $3 \times 10^7$ K, then the density contrast of $c \sim 3000$ will make them insensitive to the varying gas velocity field on spatial scales smaller than $\sim c \times x$, where $x$ is the size of the cloud. For instance, if the size of the typical cloud is

$\sim$1 pc, then it has to travel $\sim$3 kpc through the ambient gas before ram pressure will accelerate it to the velocity comparable with the gas velocity.

## 7 CONCLUSIONS

The Perseus cluster spectrum from 5 to 9 keV measured by *XMM–Newton* can be well described as emission from an optically thin plasma with solar ratios of elemental abundances, provided that the most recent version (1.3) of the APEC code is used.

The lack of any visible suppression of the He-like iron 6.7-keV line in the inner region of the Perseus cluster core implies that the optical depth of the cluster gas is significantly reduced by gas motions with velocities of the order of half the gas sound velocity. Dissipation of these motions may provide enough heat to replenish the energy lost from radiative cooling if the spatial scales of velocity variations are small enough (e.g. comparable to the size of AGN-inflated relativistic plasma bubbles).

## ACKNOWLEDGMENTS

We are grateful to Randall Smith and Nancy Brickhouse for useful discussions. We thank the editor and the referee for important comments and suggestions. WF and CJ thank MPA for its hospitality during their summer 2002 visits, as well as the Smithsonian Institution and *Chandra* Observatory for support (NASA contract NAS8-39073). This work is based on observations obtained with *XMM–Newton*, a European Space Agency (ESA) science mission with instruments and contributions directly funded by ESA Member States and the USA (NASA).

## REFERENCES

Akimoto F., Tawara Y., Furruzawa A., Kumada A., Yamashita K., 1997, in Makino F., Mitsuda K., eds, X-ray Imaging and Spectroscopy of Cosmic Hot Plasmas. Tokio, Universal Academy Press, p. 95
Akimoto F., Furuzawa A., Tawara Y., Yamashita K., 1999, AN, 320, 283
Anders E., Grevesse N., 1989, GeCoA, 53, 197
Arnaud K. A., 1996, in Jacoby G., Barnes J., eds, ASP Conf. Ser. Vol. 101, Astronomical Data Analysis Software and Systems V. Astron. Soc. Pac., San Francisco, p. 17
Böhringer H., Voges W., Fabian A. C., Edge A. C., Neumann D. M., 1993, MNRAS, 264, L25
Böhringer H. et al., 2001, A&A, 365, L181
Böhringer H. et al., 2003, A&A, to be submitted
Brüggen M., Kaiser C. R., 2002, Nat, 418, 301
Churazov E., Brüggen M., Kaiser C. R., Böhringer H., Forman W., 2001, ApJ, 554, 261
Churazov E., Sunyaev R., Forman W., Böhringer H., 2002, MNRAS, 332, 729
Churazov E., Forman W., Jones C., Böhringer H., 2003, ApJ, 590, 225
Conselice C. J., Gallagher J. S., Wyse R. F. G., 2001, AJ, 122, 2281
Dupke R. A., Arnaud K. A., 2001, ApJ, 548, 141
Fabian A. C. et al., 2000, MNRAS, 318, L65
Fabian A. C., Sanders J. S., Crawford C. S., Conselice C. J., Gallagher J. S., Wyse R. F. G., 2003a, MNRAS, 344, L48
Fabian A. C., Sanders J. S., Allen S. W., Crawford C. S., Iwasawa K., Johnstone R. M., Schmidt R. W., Taylor G. B., 2003b, MNRAS, 344, L43
Frenk C. S. et al., 1999, ApJ, 525, 554
Furusho T., Yamasaki N. Y., Ohashi T., Shibata R., Ezawa H., 2001, ApJ, 561, L165
Gastaldello F., Molendi S., 2003, Conf. on the Riddle of Cooling Flows in Galaxies and Clusters of Galaxies. Available on-line at http://www.astro.virginia.edu/coolflow/abs.php
Gilfanov M. R., Sunyaev R. A., Churazov E. M., 1987, Sov. Astron. Lett., 13, 233
Inogamov N., Sunyaev R., 2003, Astron. Lett., in press
Kaastra J. S., 1992, An X-Ray Spectral Code for Optically Thin Plasmas, updated version 2.0. Internal SRON-Leiden Report (http://www.sron.nl/divisions/hea/spex)
Landau L. D., Lifshitz E. M., 1963, Fluid Mechanics. Pergamon, Oxford
Liedahl D. A., Osterheld A. L., Goldstein W. H., 1995, ApJ, 438, L115
Mathews W. G., Buote D. A., Brighenti F., 2001, ApJ, 550, L31
Matsushita K., Finoguenov A., Böhringer H., 2003, A&A, 401, 443
Mazzotta P., Mazzitelli G., Colafrancesco S., Vittorio N., 1998, A&AS, 133, 403
Mewe R., Gronenschild E. H. B. M., van den Oord G. H. J., 1985, A&AS, 62, 197
Mewe R., Lemen J. R., van den Oord G. H. J., 1986, A&AS, 65, 511
Molendi S., Matt G., Antonelli L. A., Fiore F., Fusco-Femiano R., Kaastra J., Maccarone C., Perola C., 1998, ApJ, 499, 608
Norman M. L., Bryan G. L., 1999, in Röser H.-J., Meisenheimer K., eds, Lecture Notes in Physics 530, The Radio Galaxy Messier 87. Springer, New York, p. 106
Reynolds C. S., Heinz S., Begelman M. C., 2002, MNRAS, 332, 271
Sazonov S. Y., Churazov E. M., Sunyaev R. A., 2002, MNRAS, 333, 191
Schmidt R. W., Fabian A. C., Sanders J. S., 2002, MNRAS, 337, 71
Shigeyama T., 1998, ApJ, 497, 587
Smith R. K., Brickhouse N. S., Liedahl D. A., Raymond J. C., 2001, ApJ, 556, L91
Sunyaev R., Norman M., Bryan G., 2003, Astron. Lett., in press (astro-ph/0310041)
Verner D. A., Verner E. M., Ferland G. J., 1996, Astron. Data Nucl. Data Tables, 64, 1
Xu H. et al., 2002, ApJ, 579, 600

This paper has been typeset from a TEX/LATEX file prepared by the author.